Molecular Therapy
Nucleic Acids
Original Article

Angpt2 Induces Mesangial Cell Apoptosis through the MicroRNA-33-5p-SOCS5 Loop in Diabetic Nephropathy

Yi-Chun Tsai,[1,2,3,4,5] Po-Lin Kuo,[1] Wei-Wen Hung,[6] Ling-Yu Wu,[1] Ping-Hsun Wu,[1,5] Wei-An Chang,[1,7] Mei-Chuan Kuo,[1,2,3,5] and Ya-Ling Hsu[8]

[1]Graduate Institute of Clinical Medicine, College of Medicine, Kaohsiung Medical University, Kaohsiung, Taiwan; [2]School of Medicine, College of Medicine, Kaohsiung Medical University, Kaohsiung, Taiwan; [3]Faculty of Renal Care, College of Medicine, Kaohsiung Medical University, Kaohsiung, Taiwan; [4]Division of General Medicine, Kaohsiung Medical University Hospital, Kaohsiung, Taiwan; [5]Division of Nephrology, Department of Medicine, Kaohsiung Medical University Hospital, Kaohsiung, Taiwan; [6]Division of Endocrinology and Metabolism, Kaohsiung Medical University Hospital, Kaohsiung, Taiwan; [7]Division of Pulmonary and Critical Care Medicine, Kaohsiung Medical University Hospital, Kaohsiung, Taiwan; [8]Graduate Institute of Clinical Medicine, College of Medicine, Kaohsiung Medical University, Kaohsiung, Taiwan

Diabetic nephropathy (DN) is the leading cause of end-stage renal disease. Mesangial cell (MC) loss is correlated with worsening renal function in DN. Disturbance of angiopoietin (Angpt)/Tie ligand-receptor system causes inflammation and abnormal angiogenesis. This association between elevated circulating Angpt2 and poor renal outcome has been in DN patients. However, the pathogenic role of Angpt2 in the MCs remains unknown. We found serum Angpt2 levels were elevated in type 2 diabetes mellitus (DM) patients and db/db mice, which correlated with albuminuria. Angpt2 synergistically induced MC apoptosis under high glucose (HG), and miR-33-5p regulated Angpt2-inducing MC apoptosis treated with HG. Loss of miR-33-5p increased suppressor of cytokine signaling 5 (SOCS5), leading to the inhibition of Janus kinase 1 and signal transducer and activator of transcription 3 signaling transduction. Elevated expression of SOCS5 was found in the MCs in kidney sections of both db/db mice and type 2 DM patients. Decreased miR-33-5p levels were found in the urine of db/db mice and type 2 DM patients, and miR-33-55p levels negatively correlated with albuminuria. Angpt2 leads to MC apoptosis via the miR-33-5p-SOCS5 loop in DN. miR-33-5p is predictive of kidney injury in DN. These findings may provide future applications in predicting renal dysfunction and the therapeutic potential of DN.

INTRODUCTION

Diabetic nephropathy (DN) is the leading cause of chronic kidney disease (CKD), and it accounts for nearly 30%–50% of people requiring renal replacement therapy in the world.[1] DN results in an enormous burden on affected individuals and health-care systems. Mesangial cells (MCs) play a pivotal role in maintaining glomerular structure and function, with their contractility supporting the structure of capillary loops and modulating glomerular filtration.[2] Numerous data show that MC loss is correlated with worsening of albuminuria and renal function in DN.[3,4] Consequently, regulating MC number is a principal goal in the treatment of DN.

The angiopoietin (Angpt)/Tie ligand-receptor system tightly controls the endothelial phenotype during angiogenesis and vascular inflammation.[5] Angpt1-mediated Tie2 phosphorylation maintains structural integrity of the vasculature, protects endothelial cells from apoptosis, and inhibits permeability and inflammatory responses.[6,7] Angpt2 is expressed and stored in Weibel-Palade bodies of endothelial cells.[8] The rapid release of Angpt2 from endothelial cells occurs under activation of the endothelium by different endothelial cytokines (vascular epithelial growth factor and tumor necrosis factor) and environmental cues (hypoxia, superoxides, and high glucose).[9–11] An elevated concentration of Angpt2 disrupts Angpt1/Tie2 signaling by preventing Angpt1 from binding to the Tie2 receptor,[7,9,10] and it contributes to destabilization of the endothelium.[8] An elevated concentration of Angpt2 has been found in patients with diabetes.[12] Angpt2 not only triggers an inflammatory response[11] but also leads to pericyte loss and apoptosis in the diabetic retina.[13] Our previous study demonstrated a significant association between elevated circulating Angpt2 and rapid decline in renal function, resulting in commencing dialysis for patients with DN.[14] However, the pathophysiological mechanism of Angpt2 mediating DN, especially in MCs, is unknown.

MicroRNAs (miRNAs) are a class of small non-coding RNAs that regulate gene expression at the posttranscriptional level by binding

Received 15 August 2018; accepted 3 October 2018;
https://doi.org/10.1016/j.omtn.2018.10.003.

Correspondence: Mei-Chuan Kuo, Division of Nephrology, Department of Medicine, Kaohsiung Medical University Hospital, Kaohsiung 807, Taiwan.
E-mail: mechku@cc.kmu.edu.tw
Correspondence: Ya-Ling Hsu, Graduate Institute of Clinical Medicine, College of Medicine, Kaohsiung Medical University, Kaohsiung 807, Taiwan.
E-mail: hsuyl326@gmail.com

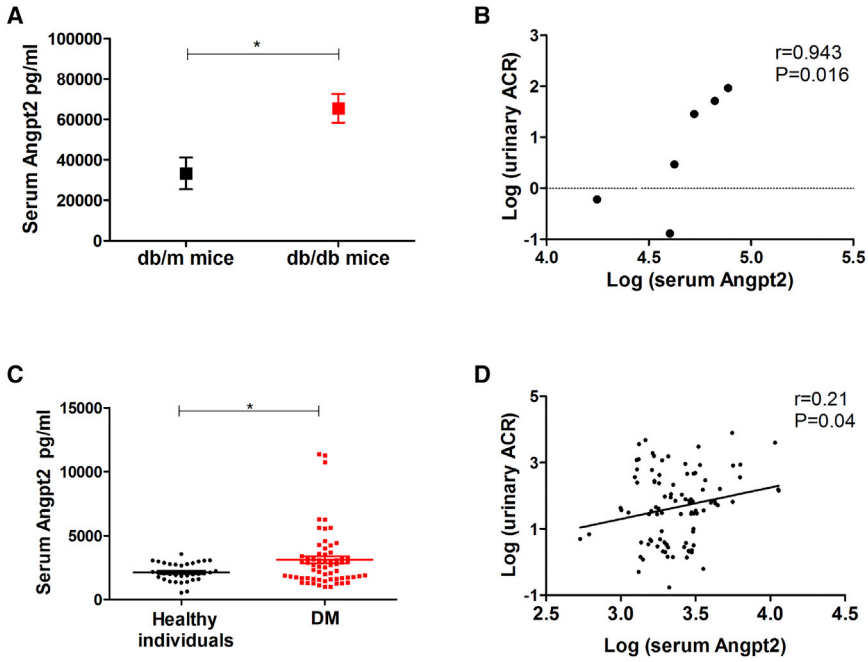

Figure 1. Serum Angiopoietin-2 Is Positively Correlated with Urinary Albumin-Creatinine Ratio in Diabetes Mellitus

(A) Serum Angiopoietin-2 (Angpt2) was more elevated in db/db mice (n = 3) than in db/m mice (n = 3). (B) A positive correlation between urinary albumin-creatinine ratio (ACR) and serum Angpt2 was found in mice. (C) Serum Angpt2 was more elevated in type 2 diabetes mellitus (DM) patients (n = 63) than in healthy individuals (n = 34). (D) A positive correlation between urinary ACR and serum Angpt2 was also found in human participants. Magnetic Luminex Assay was used to assess serum Angpt2. Urine albumin was measured using an immunoturbidimetric assay, and urine creatinine was determined by the enzymatic method. The bar graph represents the mean ± SEM. *$p < 0.05$ by two-tailed Student's t test. p value of correlation by Spearman analysis.

to target sequences within the 3′ UTR of mRNA.[15] miRNAs have been found in various organisms, and they are regarded as powerful regulators of gene expression and cellular phenotypes. They participate in a variety of biological processes, such as cell proliferation, apoptosis, hematopoiesis, and immune response, and they affect many diseases, including cancers, infectious diseases, and diabetes.[16] Accumulating data show that miRNAs are involved in the pathogenesis of DN. In mice with DN, intrarenal miR-192 and miR-377 levels were upregulated, which facilitated tissue collagen 1-alpha 1 and fibronectin production.[17,18] Higher expression of several miRNAs, such as miR-200b/c, miR-216a, and miR-217, has been detected in mouse MC treated with transforming growth factor beta 1 (TGF-β1) and in renal glomeruli from mouse models of diabetes.[19,20] The dysregulation of miRNAs can lead to DN, and, therefore, miRNAs have potential as biomarkers and predictors of clinical disease progression.[21,22] Nevertheless, what role miRNAs play in regulating the pathophysiological signal pathway of Angpt2 in DN has not yet been well explored.

We hypothesized that Angpt2 augments MC apoptosis and that miRNAs may be involved in Angpt2 mediating the signal pathway and predicting renal function in DN. We conducted this cross-disciplinary study, including human, *in vivo* and *in vitro* studies, to examine the molecular mechanisms of Angpt2 driving MC apoptosis. The results demonstrate that Angpt2 induces apoptotic cell death in MCs by miR-33-5p downregulation, which directly binds to its target, suppressor of cytokine signaling 5 (SOCS5), leading to the inhibition of the survival pathway of Janus kinase 1 (JAK1)/signal transducer and activator of transcription 3 (STAT3) in DN.

RESULTS

Increased Serum Angpt2 and a Positive Correlation between Angpt2 and Urinary Albumin-Creatinine Ratio in db/db Mice and Type 2 Diabetes Mellitus Patients

To investigate the association of kidney function with Angpt2, we examined serum and urinary Angpt2 in db/m mice (n = 3) and db/db mice (n = 3). We found that serum Angpt2 levels are higher in db/db mice than in db/m mice (Figure 1A). The positive correlation between serum Angpt2 and urinary albumin-creatinine ratio (ACR) is shown in Figure 1B.

We enrolled 63 type 2 diabetes mellitus (DM) patients and 34 healthy individuals in our study. Characteristics of the study participants are shown in Table S1. Type 2 DM patients had higher serum Angpt2 levels compared to healthy individuals (Figure 1C), and serum Angpt2 was positively correlated with urinary ACR in all study participants (Figure 1D). Besides, lower serum Angpt1 levels and a higher serum Angpt2:Angpt1 ratio were found in type 2 DM patients compared to healthy individuals (Figures S1A and S1B), and serum Angpt2:Angpt1 ratio was also positively associated with urinary ACR in all study participants (Figure S1C). There was a slight elevation of urinary Angpt2 levels in both db/db mice and type 2 DM patients, but concentrations of Angpt2 were very low (Figure S2). These results support our hypothesis that circulating Angpt2 may play a pathogenic role in DN.

Angpt2 Exhibits a Synergistic Effect on the Induction of Intrinsic Proapoptotic Pathway in Mouse Mesangial Cells through Tie2 Receptor under High Glucose Condition

MC apoptosis has been found in DN, which correlates with worsening albuminuria.[3,4] Thus, we determined whether Angpt2 reinforces cell death in MCs under a high-glucose (HG) condition. Angpt2 alone decreased mouse MC (MMC) viability under a normal-glucose (NG) condition (Figure 2A). HG reduced cell viability of MMCs, and Angpt2 aggravated the decrease in cell

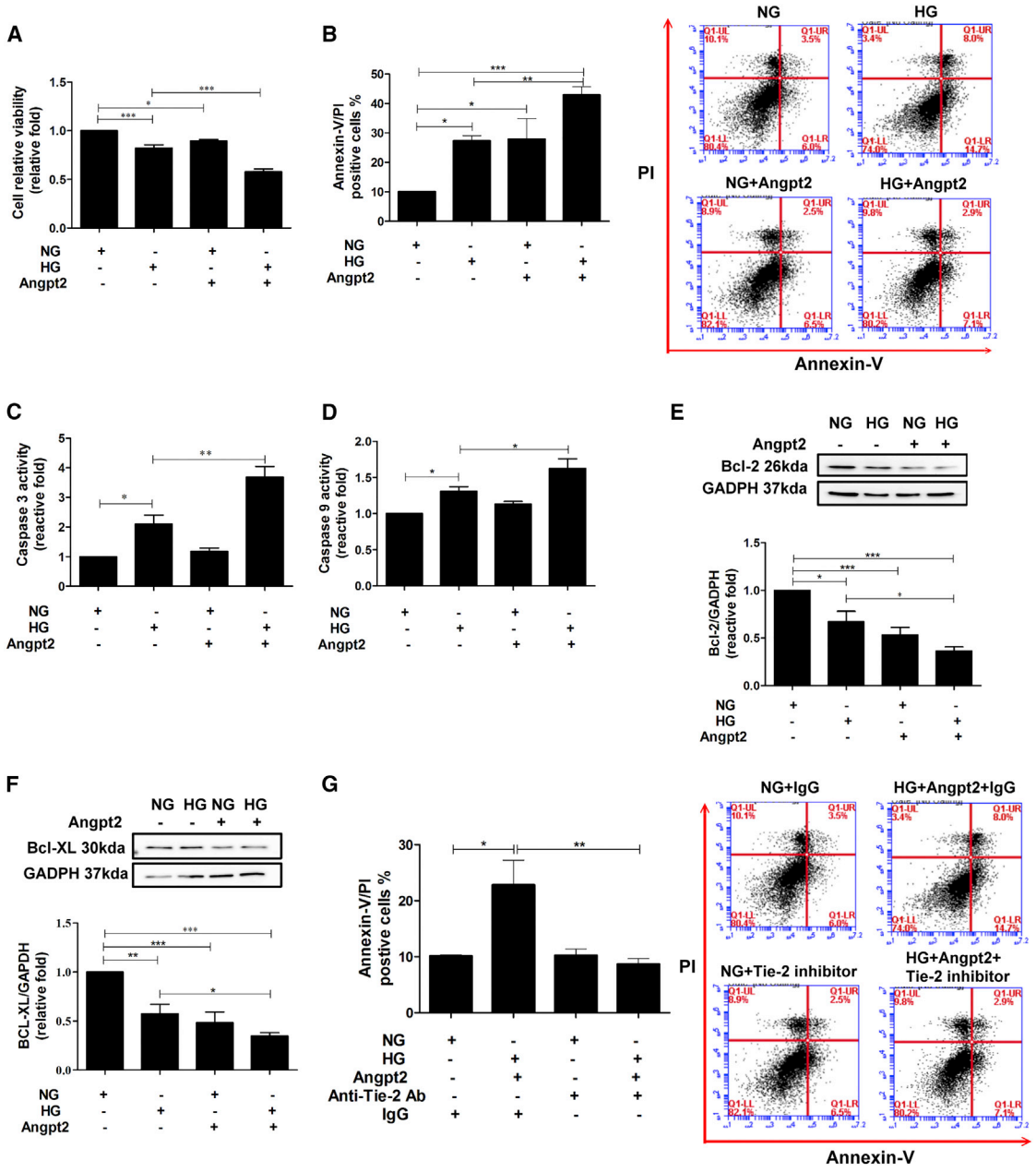

Figure 2. Angpt2 Exhibits a Synergistic Effect on the Induction of Apoptosis in Mouse Mesangial Cells through Tie-2 Receptor under a High Glucose Condition

(A) The effect of Angpt2 on cell viability of mouse mesangial cells (MMCs). MMCs were incubated for 48 hr with or without Angpt2 (300 ng/mL) under normal glucose (NG, 5.5 mM) or high glucose (HG) (25 mM) condition. Cell viability was assessed by WST-1 assay. (B) Angpt2 enhanced cell death under an HG condition in MMCs. MMCs were double stained with Annexin-V fluorescein isothiocyanate and PI and analyzed by flow cytometry. Cell apoptosis was expressed as the percentage of cells with Annexin-V and PI double staining in total cell populations. (C and D) Angpt2 aggravated caspase-3 (C) and caspase-9 (D) activation in MMCs treated with HG for 48 hr. (E and F) Angpt2 reduced B cell lymphoma 2 (Bcl-2) (E) and B cell lymphoma-extra large (Bcl-XL) (F) protein expression in MMCs under HG for 36 hr. The activities of caspase-3 and caspase-9 were detected by fluorescent caspase assay kits. Bcl-2 and Bcl-XL protein levels were assessed by western blotting. (G) Tie2 receptor involves Angpt2-mediated apoptosis in MMCs under an HG condition. MMCs were pre-incubated either with Tie2 antibody (5 μg/mL) or IgG (5 μg/mL) for 2 hr and treated with Angpt2 for another 48 hr under an HG condition. The bar graph represents the mean ± SEM of at least three independent experiments. *$p < 0.05$, **$p < 0.01$, and ***$p < 0.001$ by ANOVA followed by the post hoc test adjusted with a Tukey correction.

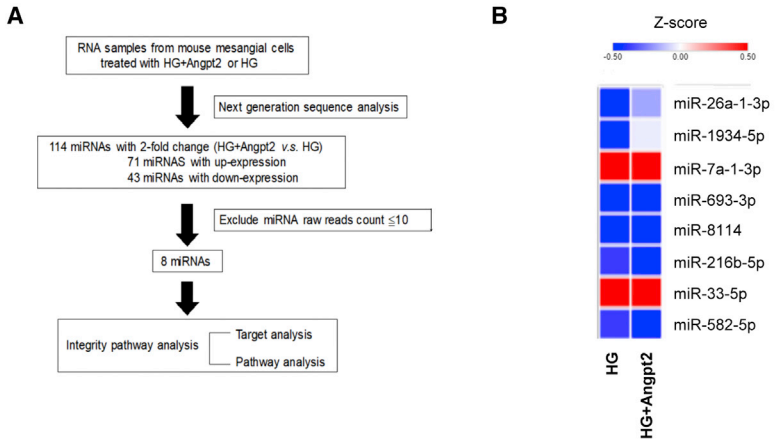

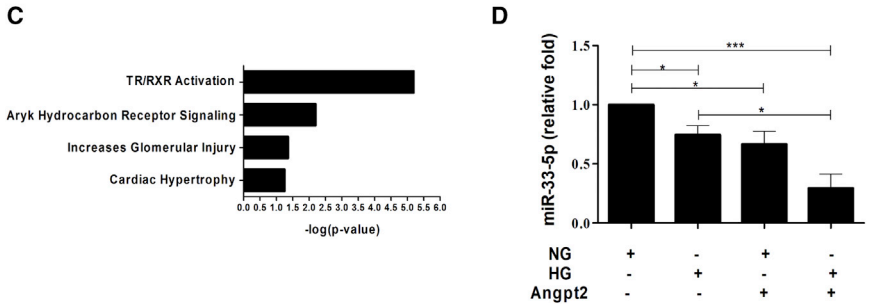

Figure 3. Identification of Potential miRNAs Contributing to Angpt2-Mediated Apoptosis in MMCs under an HG Condition

(A) The flowchart of miRNA identification and selection. (B) The heatmap revealed differentially expressed miRNAs from MMCs treated with HG + Angpt2 or HG with *Z* score values. The *Z* score of each miRNA is its expression level's relationship to the mean of expression levels of all miRNAs. (C) Ingenuity Pathway Analysis (IPA) of miR-33-5p profiles of Angpt2-treated MMCs under an HG condition. (D) miR-33-5p levels in MMCs. MMCs were treated with or without Angpt2 under an NG or HG condition for 12 hr. miR-33-5p levels were assessed by real-time qPCR. The bar graph represents the mean ± SEM of at least three independent experiments. *$p < 0.05$ and ***$p < 0.001$ by ANOVA followed by the post hoc test adjusted with a Tukey correction.

viability under the HG condition. Next, MMC apoptosis was examined by Annexin-V/propidium iodide (PI) double staining using flow cytometry. HG caused MMC apoptosis (Figure 2B). As expected, Angpt2 significantly induced MMC apoptosis alone under an NG condition, and Angpt2 aggravated MMC apoptosis under an HG condition at 48 hr. Similarly, caspase-3 activity increased in MMCs under an HG condition, and Angpt2 augmented caspase-3 activation in MMCs treated with HG (Figure 2C). These findings show that Angpt2 plays a synergistic role in MMC apoptosis under an HG condition.

HG has been proven to evoke an intrinsic proapoptotic signaling pathway in MCs.[4] As expected, caspase-9 activity increased in MMCs under an HG condition at 36 hr (Figure 2D). Angpt2 augmented caspase-9 activity in MMCs treated with HG. Western blot studies also confirmed that Angpt2 induced an MMC apoptotic pathway with the decrease in B cell lymphoma 2 (Bcl-2) and B cell lymphoma-extra large (Bcl-XL) under NG and HG conditions at 36 hr (Figures 2E and 2F).

Elevated Angpt2 disrupts Angpt1/Tie2 signaling by preventing Angpt1 from binding to the Tie2 receptor.[7,9,10] To investigate the binding receptor of Angpt2, anti-Tie2 antibody was used to determine the role of Tie2 receptor in Angpt2-induced apoptosis in MMCs. As shown in Figure 2G, Angpt2 increased the apoptosis of MMCs under an HG condition, and anti-Tie2 antibody prevented the synergistic effect of Angpt2 on apoptosis induction in MMCs. This result indicates that Tie2 is the major receptor contributing to Angpt2-mediated apoptosis in MMCs under an HG condition.

Identification of Potential miRNA in Angpt2-Treated MMCs under an HG Condition

Increasing evidence has revealed that miRNAs participate in the pathophysiologic mechanisms of DN.[17–20] Based on our findings, Angpt2 caused MMC apoptosis and was correlated with the severity of albuminuria in human beings. Thus, we investigated whether Angpt2 induced MMC apoptosis via miRNAs. The flowchart of identification of potential miRNAs is shown in Figure 3A. The profiles of small RNA from MMCs treated with HG or HG + Angpt2 for 48 hr were analyzed by next-generation sequencing (NGS). There were 114 miRNAs with significant fold changes of MMCs treated with HG + Angpt2, when compared with those treated with HG. Of 114 miRNAs, 71 miRNAs were upregulated and 43 miRNAs were downregulated. We excluded miRNAs with raw read counts ≤ 10. Finally, eight significant miRNAs were represented by heatmap, and the pathophysiologic function of their targets was analyzed by Ingenuity Pathway Analysis (IPA).

Of eight miRNAs, we found miR-33-5p expression was decreased in MMCs treated with both HG and Angpt2, when compared to those treated with HG only (Figure 3B), and this finding correlated with glomerular injury according to IPA (Figure 3C). Furthermore, RT-PCR was utilized to examine miR-33-5p expression in MMCs. miR-33-5p expression decreased in MMCs treated with HG, and Angpt2 caused a greater decrease in miR-33-5p expression in MMCs treated with HG at 12 hr (Figure 3D). These data show that miR-33-5p may participate in the synergistic effect of Angpt2 on apoptosis induction in MMCs.

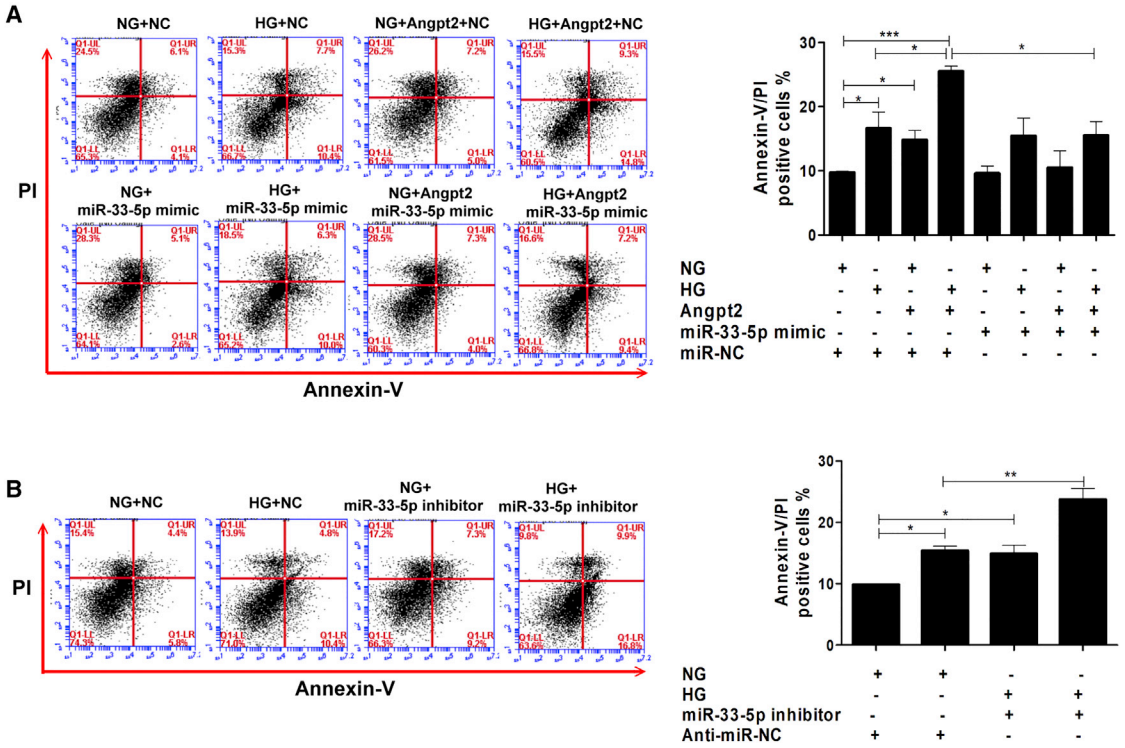

Figure 4. Angpt2-Induced MMC Apoptosis Is Mediated by miR-33-5p Inhibition under an HG Condition

(A) miR-33-5p mimics prevent the synergistic effect of Angpt2 on apoptosis induction in MMCs under an HG condition. MMCs were transfected with either miR-33-5p mimic (200 nM) or control of mimic (miR-NC, 200 nM) for 24 hr and treated with Angpt2 (300 ng/mL) under an NG or HG condition for 24 hr. Apoptotic cells were assessed by flow cytometry with Annexin-V/PI double staining. (B) miR-33-5p inhibitor mimicked the effect of Angpt2 on apoptosis induction in MMCs under an HG condition. MMCs were transfected with miR-33-5p inhibitor (50 nM) or control of inhibitor (anti-miR-NC, 50 nM) for 24 hr and then incubated under an NG or HG condition for 24 hr. The bar graph represents the mean ± SEM of at least three independent experiments. *$p < 0.05$, **$p < 0.01$, and ***$p < 0.001$ by ANOVA followed by the post hoc test adjusted with a Tukey correction.

Angpt2 Induces MMC Apoptosis by miR-33-5p Inhibition under an HG Condition

To examine the role of miR-33-5p in Angpt2-induced MMC apoptosis under an HG condition, we used miR-33-5p mimic and inhibitor to assess the proapoptotic effect of Angpt2 on MMCs. As shown in Figure 4A, miR-33-5p mimic reversed Angpt2-induced apoptosis in MMCs under an HG condition. Conversely, miR-33-5p inhibitor mimicked the effect of Angpt2 on apoptosis induction in MMCs under an HG condition (Figure 4B). These results support our hypothesis that Angpt2 induces MC apoptosis through miR-33-5p inhibition under an HG condition.

SOCS5 as a Direct Target of miR-33-5p

Since Angpt2 caused MMC apoptosis by the modulation of miR-33-5p, we further examined the miR-33-5p downstream target, which contributes to Angpt2-mediated apoptosis in MMCs. We conducted bioinformatic predictions using miRmap and TargetScan (version 7.1). These two databases indicated that the 3′ UTR of SOCS5 contains the target seed sequence against miR-33-5p, which is conserved among humans, mice, and rabbits (Figure 5A). The species-conserved miR-33-5p seed sequence in the 3′ UTR of SOCS5 is shown in Figure 5B.

miR-33-5p mimics reduced luciferase activity of SOCS5-3′ UTR plasmid when compared to control mimic transfection (Figure 5C). miR-33-5p inhibitor increased SOCS5 levels, mimicking the effect of HG and Angpt2 in MMCs (Figure 5D). miR-33-5p mimic prevented the upregulation of SOCS5 in MMCs treated with either NG or HG (Figure 5E). HG increased the expression of SOCS5 in MMCs, and Angpt2 potentiated SOCS5 upregulation in MMCs under an HG condition at 24 hr (Figure 5F). In addition, levels of SOCS5 protein expression were higher in the MCs of kidney sections of diabetic db/db mice than in those of C57BL/6 mice and non-diabetic db/m mice (Figure 5G). More importantly, immunohistochemistry (IHC) stain also revealed that levels of SOCS5 were greater in the MCs of kidney sections of type 2 DM patient than in those of upper tract urothelial carcinoma (UTUC) patients with normal kidney function and normal glomerulus (Figure 5H). Thus, Angpt2 increases SOCS5 expression by miR-33-5p inhibition, and SOCS5 may participate in Angpt2 mediating the signal pathway of DN.

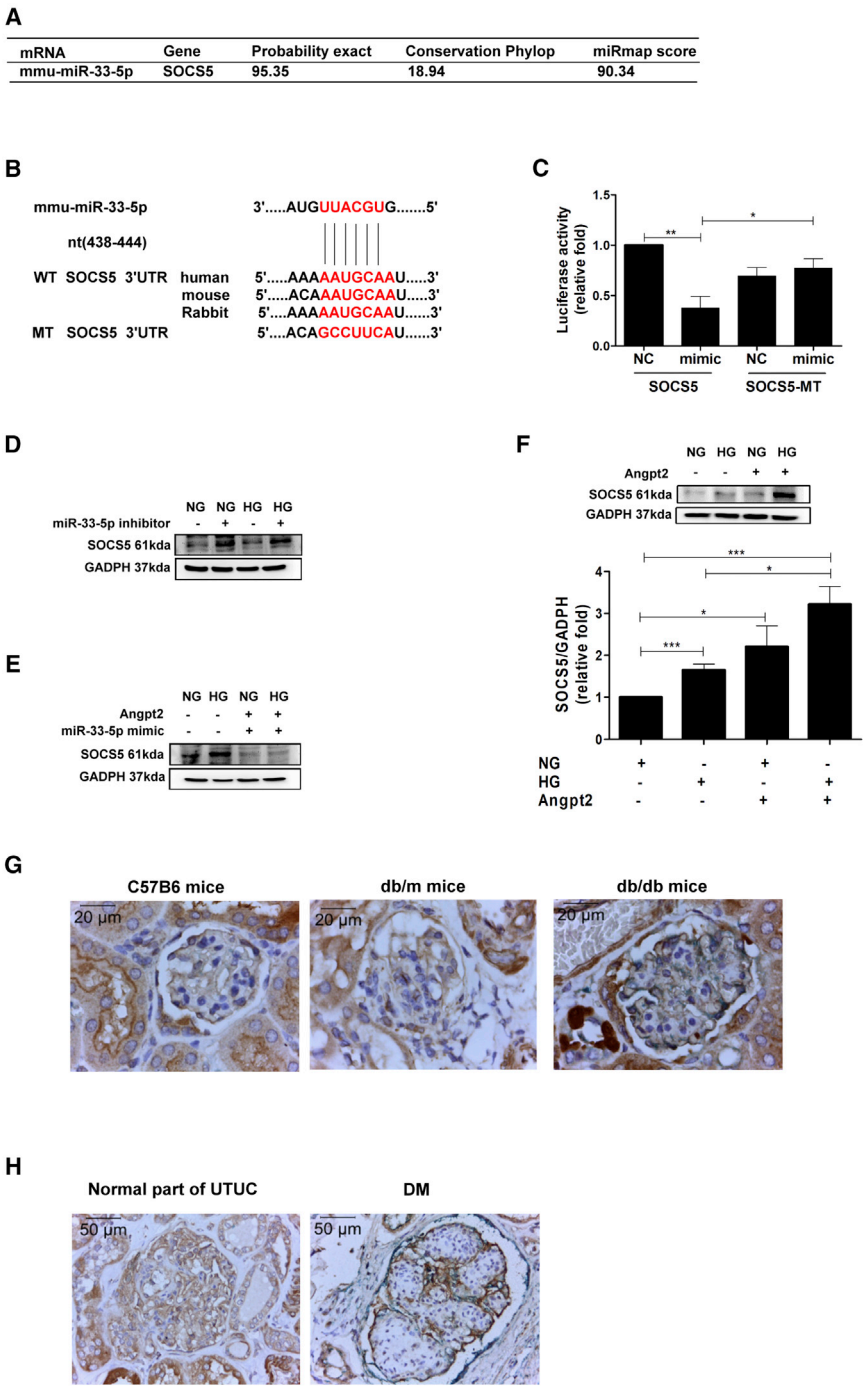

Figure 5. Suppressor of Cytokine Signaling 5 Is a Direct Target of miR-33-5p in MMCs

(A) The predictive binding score of miR-33-5p and suppressor of cytokine signaling 5 (SOCS5) mRNA according to miRmap database. (B) A schematic representation of sequence alignment of SOCS5 mRNA 3′ UTR based on TargetScan 7.1 version. (C) Luciferase activity was repressed by endogenous miR-33-5p. HEK293 cells were cotransfected with pGL3-SOCS5-3′ UTR luciferase plasmid/pRL-TK Renilla (1:8) or pGL3-SOCS5-3′ UTR MT luciferase plasmid/pRL-TK Renilla (1:8) with various miRNA mimics (control mimic or miR-33-5p mimic) by DharmaFECT Duo transfection reagent after 48 hr, and both firefly and Renilla luciferase activities were quantified using the Dual-Glo Luciferase Assay System. Endogenous SOCS5 in MMCs was regulated by miR-33-5p under an HG condition. (D and E) miR-33-5p inhibitor (D) enhanced and miR-33-5p mimic (E) suppressed SOCS5 expression in MMCs under an NG or HG condition. Cells were transfected with either miR-33-5p inhibitor or miR-33-5p mimic, and, 24 hr after transfection, the cells were treated with Angpt2 for 24 hr under an NG or HG condition. Western blotting was utilized to measure SOCS5 protein expression. (F) Angpt2 increased SOCS5 expression in MMCs under an NG condition, and it augmented SOCS5 expression in MMCs under an HG condition. Western blotting and quantitative analysis of SOCS5 was performed in MMCs treated with Angpt2 under NG or HG for 24 hr. (G and H) The expression of SOCS5 in the MCs of kidneys in mice (G) and humans (H). The kidney sections of C57BL/6 mice, non-diabetic db/m mice, diabetic db/db mice, and human donors (upper tract urothelial carcinoma, UTUC with normal kidney function and normal glomerulus) and patients with DN were co-stained with SOCS5 (brown) and α-SMA (green). The bar graph represents the mean ± SEM of at least three independent experiments. *$p < 0.05$, **$p < 0.01$, and ***$p < 0.001$ by ANOVA followed by the post hoc test adjusted with a Tukey correction.

Angpt2 Augments MMC Apoptosis through JAK1/STAT3 Pathway Inhibition by SOCS5 Upregulation under an HG Condition

SOCS5 has been regarded as an intracellular negative regulator of JAK/STAT signaling, which regulates cellular survival and proliferation.[23] Thus, we investigated whether the SOCS5-JAK1-STAT3 regulatory loop is involved in Angpt2-mediated MMC apoptosis of DN. Western blotting showed both phospho-JAK1:JAK1 and phospho-STAT3:STAT3 ratios decreased in MMCs treated with HG at 24 hr (Figures 6A and 6B). Angpt2 not only decreased phospho-JAK1:JAK1 and phospho-STAT3:STAT3 ratios in MMCs under an NG condition but also it aggravated the decrease in phospho-JAK1:JAK1 and phospho-STAT3:STAT3 ratios in MMCs under an HG condition. Moreover, we silenced SOCS5 by small interfering RNA (siRNA) transfection in MMCs, and we found that the effect of Angpt2 on apoptosis induction was prevented by SOCS5 siRNA (Figures 6C and 6D). Thus, Angpt2 causes MC apoptosis through SOCS5 upregulation, which in turn decreases JAK1/STAT3 activation.

Urinary miR-33-5p Levels Are Negatively Correlated with Serum Angpt2 Levels and Urine ACR in Mice and Type 2 DM Patients

Our *in vitro* study demonstrated that Angpt2 induces MMC apoptosis through miR-33-5p inhibition under an HG condition. We further applied our hypothesis in animal and human studies. We also examined urinary miR-33-5p expression in db/m mice (n = 3) and db/db mice (n = 3). The db/db mice had less urinary miR-33-5p expression than the db/m mice (Figure 7A), and urinary miR-33-5p levels were negatively correlated with urinary ACR and serum Angpt2 in mice (Figures 7B and 7C). Furthermore, type 2 DM patients also had lower urinary miR-33-5p levels when compared to normal individuals (Figure 7D). Study participants with the quartile 1 of urinary miR-33-5p level had higher urinary ACR and serum Angpt2 levels than those with quartile 4 of urinary miR-33-5p levels (Figures 7E and 7F). Consistent with the results of the *in vitro* study, miR-33-5p participates in the mechanism of Angpt2-mediated kidney injury, and urinary miR-33-5p has the potential for predicting kidney dysfunction.

DISCUSSION

DN is the leading cause of end-stage renal disease worldwide.[1,24] It is very important to detect the early signs of DN and prevent it from progressing to end-stage renal disease. In this cross-disciplinary study, we found that serum Angpt2 is elevated in both db/db mice and type 2 DM patients and is correlated with the severity of albuminuria. Angpt2 synergistically induces MMC apoptosis under an HG condition via an intrinsic proapoptotic pathway, which is triggered by miR-33-5p downregulation. miR-33-5p downregulation leads to increases in SOCS5, resulting in the inhibition of cell survival JAK1 and STAT3 signaling transduction. Decreased levels of miR-33-5p are found in the urine of db/db mice. Furthermore, we demonstrate that urinary miR-33-5p levels negatively correlate with kidney function in type 2 DM patients. Therefore, we have gained new insights into understanding the unique regulation of Angpt2-miR33-5p that accounts for DN development in type 2 DM patients (Figure 8).

Our previous study has demonstrated that Angpt2 is an independent predictor of rapid renal function decline and the need for commencing dialysis in DN patients.[14] Circulating Angpt2 levels can reflect the severity of renal injury in DM. Upregulation of Angpt2 was also found in a mouse model of streptomycin-induced DN.[25,26] Elevated Angpt2 levels contribute deregulating capillary growth and structural features, resulting from the effect of Angpt2 on endothelial cell junction destabilization, lumen enlargement, and endothelial cell-pericyte disruption.[27] In addition, specific overexpression of Angpt2 in podocytes causes glomerular endothelial cell apoptosis.[28] In this study, we have found that Angpt2 has a synergistic effect on apoptosis induction in MCs under an HG condition, whereas MCs are known to play a crucial role in maintaining the structure and function of the glomerular filtration barrier.[2] Angpt2 decreases the expression of antiapoptotic Bcl-2 and Bcl-XL proteins in favor of caspase-9 and caspase-3 activation. Also, blockade of Tie2 by neutralization antibody prevents the synergistic effect of Angpt2 on MC apoptosis under an HG condition, providing Tie2 a new role in the MC survival regulation. Significantly, higher circulating Angpt2 is found in both diabetic mice and type 2 DM patients, and elevated circulating Angpt2 is associated with higher albuminuria, as an early marker of DN. We believe upregulated Angpt2 is involved in the disruption of the glomerular filtration barrier, thereby resulting in renal injury in DM.

Angpt2 mediates the cross-talk between glomerular endothelial cells (GECs) and podocytes, resulting in renal dysfunction.[29] Vascular endothelial cells have been claimed as the primary source of Angp2.[30,31] In our Supplemental Information, HG increases Angpt2 mRNA in GECs (Figure S3A), but very low levels of Angpt2 protein can be detected in the supernatant of GECs treated with HG (Figure S3B). Urinary Angpt2 levels are also undetectable in both diabetic mice and type 2 DM patients with high circulating Angpt2 levels (Figure S2). Therefore, we suppose systemic circulating Angpt2, not local production of Angpt2 in the kidney microenvironment, contributes to MC apoptosis in DN.

Emerging evidence indicates that miRNAs are dysregulated in kidneys, contributing to adverse DN progression.[32,33] Exploring their role and regulatory network in the course of DN progression enables physicians to restrict the loss of renal function. The combination of NGS and IPA confirms that miR-33-5p has potential predictive activity of glomerular injury. Previous studies have reported that miR-33 deficiency inhibits proliferation and fibrosis through the TGF-β/Smad pathway in cardiac fibroblasts.[34] However, whether miR-33 affects MCs under an HG condition is as yet unknown. We found that HG slightly decreases miR-33-5p levels in MCs while Angpt2 dramatically reduces miR-33-5p level in MCs under an HG condition. miR-33-5p inhibitor imitates the synergistic effect of Angpt2 on apoptosis induction in MCs under an HG condition, whereas miR-33-5p mimic prevents Angpt2-induced MC apoptosis under an HG condition. Considering that miR-33 levels are decreased in the urine of patients with type 2 DM and these decreased urine levels are positively associated with serum Angpt2 proangiogenic activity, this suggests that miR-33 might be one of the key factors for Angpt2-derived DN progression and miR-33-5p may have a therapeutic effect on DN.

miRNAs are secreted into the circulation by various mechanisms, such as exosomes, microvesicles, or apoptotic bodies.[35] Because of the stability of miRNAs, they can be quantified in plasma, serum, or body fluids, including urine. Urinary miRNAs have been considered as biomarkers for renal injury.[21,35] Thus, to examine the predictive activity of miRNAs in renal injury due to DM, we measured urinary miR-33-5p levels in mice and humans. Our findings show that not only type 2 DM patients but also diabetic mice have lower miR-33-5p levels in the urine, and low urinary miR-33-5p is correlated with a high urinary ACR. In addition to the potential therapeutic effect, we think that miR-33-5p is a useful biomarker that can predict the severity of renal injury in DN, enabling clinical physicians to detect early signs of onset or the adverse progression of DN.

The SOCSs have been identified as crucial negative regulators of various cytokines employing JAK/STAT signaling, regulating genes

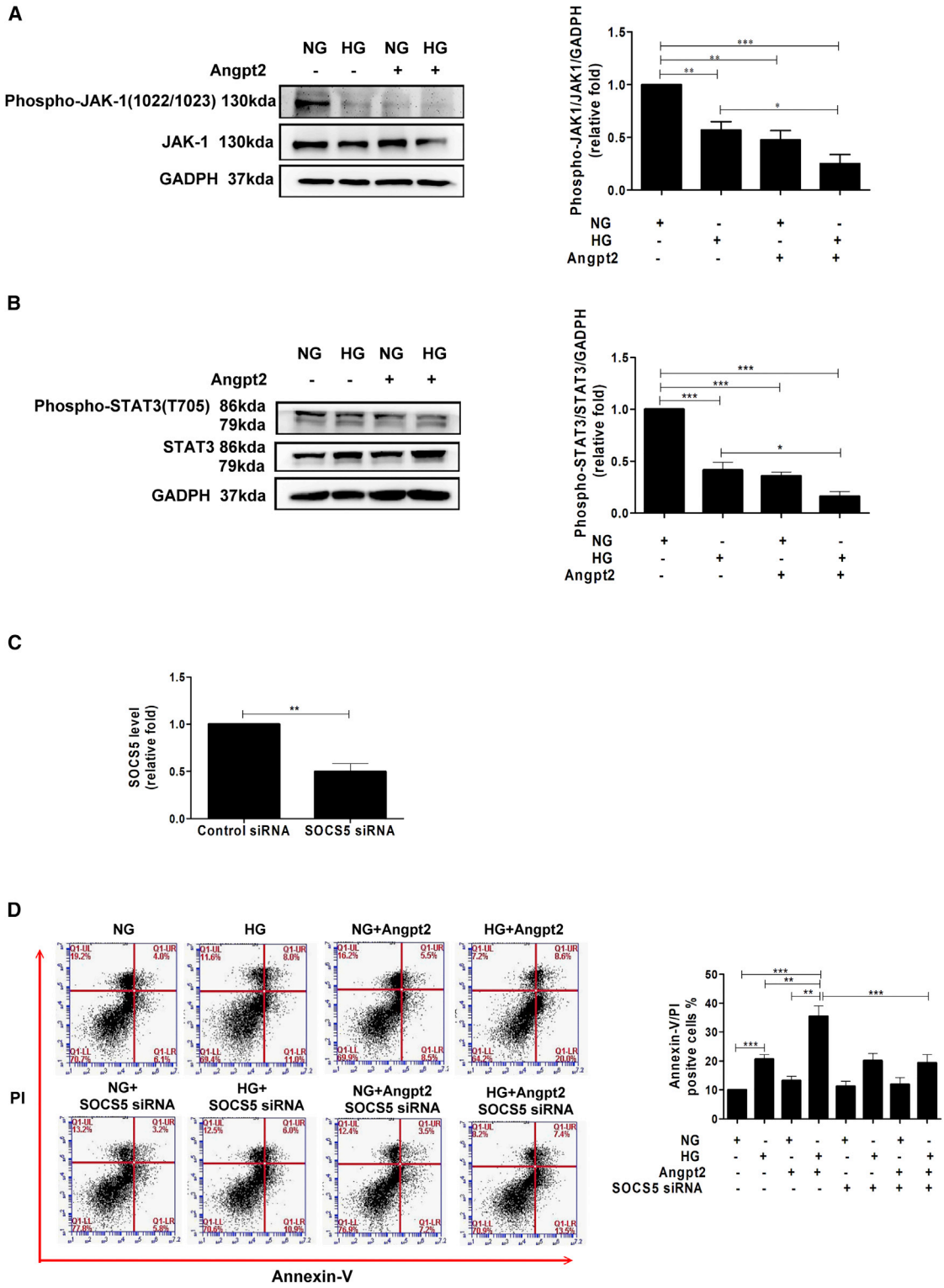

Figure 6. Angpt2 Induced MMC Apoptosis through the SOCS5/JAK1/STAT3 Pathway under an HG Condition

(A and B) Angpt2 reduced the phosphorylated JAK1:JAK1 ratio (A) and phosphorylated STAT3:STAT3 ratio (B) in MMCs under an NG condition, and it aggravated both reductions in MMCs under an HG condition. Western blotting and quantitative analysis of phosphorylated Janus kinase 1 (JAK1), total JAK1, phosphorylated signal

(legend continued on next page)

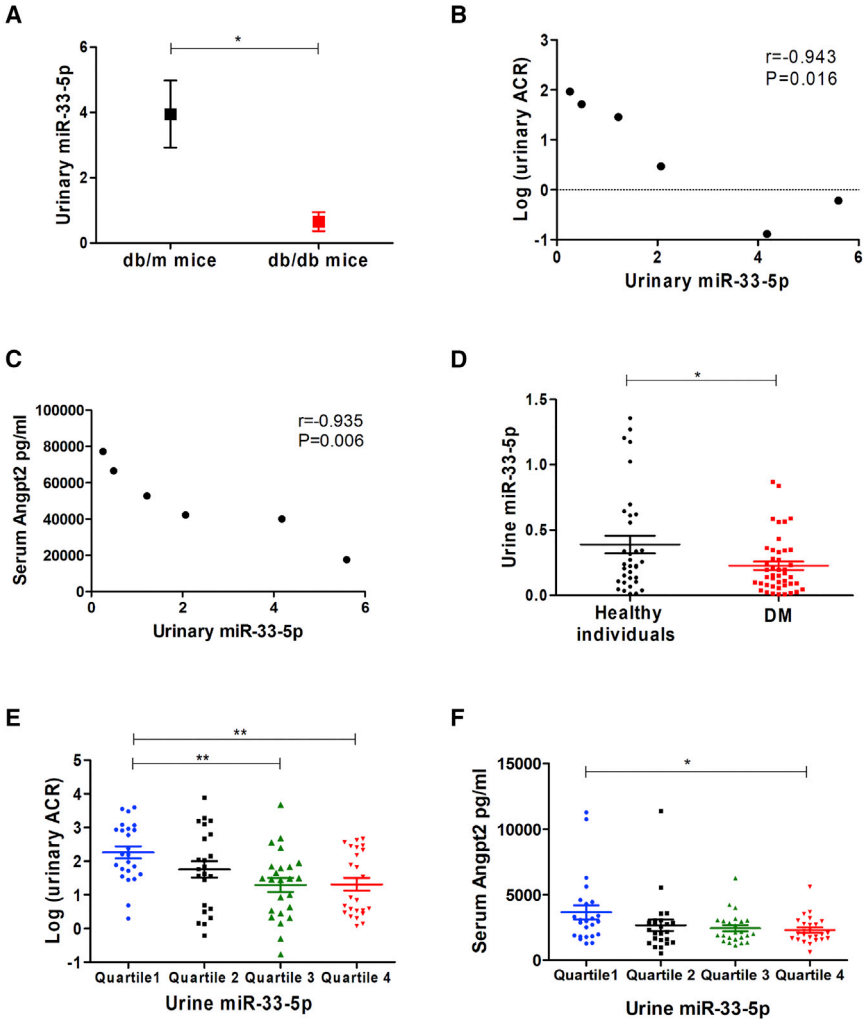

Figure 7. Urinary miR-33-5p Is Negatively Correlated with Renal Dysfunction and Serum Angpt2 in Mice and Humans

(A) Urinary miR-33-5p levels were lower in db/db mice (n = 3) compared to db/m mice (n = 3). (B and C) Urinary miR-33-5p was negatively correlated with urinary ACR (B) and serum Angpt2 (C) in mice. (D) Urinary miR-33-5p levels were lower in type 2 DM patients (n = 63) compared to healthy individuals (n = 34). (E and F) Urinary miR-33-5p levels were negatively correlated with urinary ACR (E) and serum Angpt2 (F) in human participants. Extracellular vesicular miR-33-5p in the urine of mice and humans was isolated and then assessed by real-time qPCR. Magnetic Luminex Assay was used to assess serum Angpt2. Urine albumin was measured using an immunoturbidimetric assay, and urine creatinine was determined by the enzymatic method. The bar graph represents the mean ± SEM. *p < 0.05 and **p < 0.01 by Student's t test or ANOVA followed by the post hoc test adjusted with a Tukey correction, and p value of correlation was analyzed by Spearman analysis.

involved in cellular differentiation, proliferation, inflammation, and fibrosis.[23,36] Previous studies have reported that HG induces apoptosis in retinal epithelial cells and pancreas β cells by promoting SOCS1 signaling.[37,38] Ortiz-Muñoz et al.[36] have pointed out that SOCS1 and SOCS3 expression increases in diabetic rats. HG induces SOCS1 and SOCS3 expression, and SOCS1 and SOCS3 overexpression diminishes HG-induced STAT1 and JAK2 tyrosine phosphorylation in MCs.[36]

In contrast to SOCS1 and SOCS3, the role of SOCS5 in DN progression remains largely unclear. Our study identifies miR-33-5p as a major regulator of SOCS5, suggesting that it is one mechanism associated with apoptotic cell death in MCs, leading to DN progression. Our results show that HG increases SOCS5 levels in MCs and that Angpt2 dramatically enhances the expression of SOCS5 in MCs, consistent with the synergistic effect of Angpt2 on apoptosis induction. Increased SOCS5 is associated with the inactivation of JAK1 and STAT3 in MCs. Inhibition of SOCS5 by siRNA transfection suppresses Angpt2-induced apoptotic cell death. The pathological role of SOCS5 is also supported by increased levels of SOCS5 in the MCs of kidneys in DM mice and type 2 DM patients. Consequently, we believe Angpt2 induces apoptosis in MCs through the SOCS5/JAK1/STAT3 pathway under miR-33-5p regulation within an HG environment. The pathway of Angpt2-miR-33-5p has the potential to be a therapeutic target of DN in the future.

In conclusion, we demonstrate that Angpt2 induces MC apoptosis via an intrinsic proapoptotic pathway under an HG condition. Angpt2-driven MC apoptosis is mediated by the miR-33-5p-SOCS5 loop. miR-33-5p is predictive of the severity of kidney injury in DN. This study provides future applications in the prediction of DN prognosis and a therapeutic potential of DN. We hope these findings will assist in understanding the mechanisms and clinical care of DN.

transducer and activator of transcription 3 (STAT3), and total STAT3 were performed in MMCs treated with Angpt2 under an NG or HG condition for 24 hr. (C) Efficacy of SOCS5 siRNA in MMCs. (D) SOCS5 siRNA prevented Angpt2-induced apoptosis in MMCs under an HG condition. Cells were transfected with SOCS5 siRNA, and, 24 hr after transfection, the cells were treated with Angpt2 for 48 hr under an NG or HG condition. Apoptotic cell counts were assessed by flow cytometry with Annexin-V/PI double staining. The bar graph represents the mean ± SEM of at least three independent experiments. *p < 0.05, **p < 0.01, and ***p < 0.001 by Student's t test or ANOVA followed by the post hoc test adjusted with a Tukey correction.

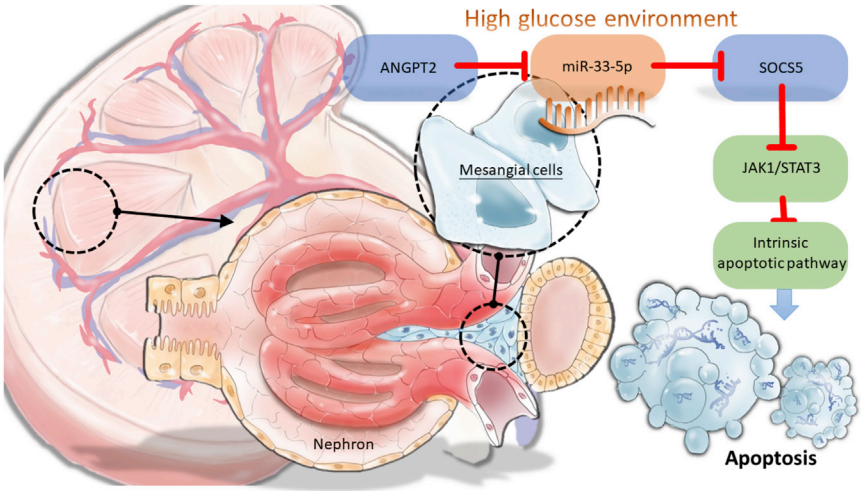

Figure 8. Illustration of the Mechanism of Angpt2-Induced Apoptosis in MCs through the miR-33-5p-SOCS5 Loop in DN

MATERIALS AND METHODS

Reagents and Antibodies

Recombinant mouse Angpt2 proteins (7186-AN), anti-Mouse/Rat Tie2 antibody (AF762), and control polyclonal Goat immunoglobulin G (IgG) (AB-108-C) were purchased from R&D Systems (USA). Antibodies against STAT3 (9139), phospho-STAT3 (Tyr705) (9131), JAK1 (3332), phospho-JAK1 (Tyr1034/1035) (3331S), Bcl-XL (2762), and Bcl-2 (3498); Annexin/PI kits (6592) and caspase-3 activity assay kit (5723); and anti-rabbit (7074S)/mouse (7076S) IgG horseradish peroxidase (HRP)-linked antibody were obtained from Cell Signaling Technology (USA). Caspase-9 activity assay kit (K119) was purchased from BioVision Technologies (USA). GAPDH antibody (MAB374) was obtained from Millipore. SOCS5 antibody (PA1-41253) was obtained from Thermo Fisher Scientific (USA).

Human Study Participants

We enrolled 63 type 2 DM patients, with estimated glomerular rate $\geq$30 mL/min/1.73 m^2, and 34 healthy volunteers in the study. Study participants were asked to fast for at least 12 hr before urine and blood sample collection. All urine and blood samples were aliquoted and stored in a −80°C freezer.

We also collected samples of kidney tissues from four DN patients scheduled for kidney biopsies and four patients receiving nephrectomy because of UTUC. This study was approved by the Institutional Review Board of the Kaohsiung Medical University Hospital (KMUHIRB-G[II]20150044, KMUHIRB-G[I]20160036, and KMUHIRB-20130089).

Experimental Animals

The 5-week-old male C57BL/6 mice, pathogen-free male db/m mice (non-diabetic animal model), and db/db mice (type 2 DM animal model) were purchased from the National Laboratory Animal Center in Taiwan. At the 12th week, we collected blood and urine samples and then harvested the kidneys. The kidneys were fixed in 4% paraformaldehyde. All animal experiments in this study were in strict agreement with Kaohsiung Medical University and Use Committee.

Quantification of Serum and Urinary Angpt2 and Angpt1 and Urinary ACR in Humans and Mice

Levels of Angpt2 and Angpt1 in serum and urine of humans and mice were measured using Magnetic Luminex Assay (LXSAHM, R&D Systems, USA). Levels of urinary albumin in humans and mice were measured using immunoturbidimetric assay with Tina-quant Albumin Gen.2 (ALBT2, Roche, USA). Concentrations of urine creatinine in humans and mice were measured using the enzymatic method (creatinine plus version 2, CREP2, Roche, USA).

Cell Line and Cell Culture

MMCs (CRL1927) and HEK293 cells were purchased from the American Type Culture Collection. MMCs were cultured in growth media of DMEM with NG (5.5 mM; Gibco, USA), supplemented with 5% fetal bovine serum (FBS). HEK293 cells were cultured in DMEM containing 10% FBS. All experiments treated MMCs with NG (5.5 mM) or HG (25 mM; Lonza, Switzerland) in cell culture medium containing 1% FBS.

Cell Viability Assay

The viability of MMCs was determined by using WST-1 Cell Proliferation Assay (Clontech Laboratories, Mountain View, CA, USA). MMCs (5×10^3 cells/well) were seeded in 96-well plates for 24 hr. Cells were cultured under NG or HG conditions, with or without mouse recombinant Angpt2 protein (300 ng/mL), for 48 hr. Cells were incubated with WST-1 substrate at 37°C for 1 hr, and absorbance at 450 nm was detected using an ELISA reader.

RNA Sequencing

MMCs were cultured in an HG condition with or without mouse recombinant Angpt2 protein (300 ng/mL) for 48 hr. Expression profiles of miRNAs of cells were performed with NGS. Total RNA from harvested cells was extracted by Trizol Reagent (Invitrogen, USA), and it was readied for further RNA preparation and sequencing analysis of small RNA sequencing (RNA-seq) by Welgene Biotechnology (Taipei, Taiwan). The quality of extracted RNA was confirmed by RNA integrity number (RIN) using an Agilent Bioanalyzer (Agilent Technologies, USA).

To construct the small RNA library and perform deep sequencing, samples were prepared using an Illumina sample preparation kit

according to the TruSeq Small RNA Sample Preparation Guide. Total RNA was ligated with 3′ and 5′ adapters and reverse transcribed into cDNA by PCR amplification. The harvested cDNA constructs were fractionated by size on a 6% PAGE, and the bands containing 18- to 40-nt RNA fragments (140–155 nt in length with both adapters) were purified. Libraries were then sequenced on an Illumina GAIIx instrument (50-cycle single read), and the sequencing results were processed with the Illumina software. The criteria for differentially expressed miRNAs between cells cultured in HG with Angpt2 and HG only were set at fold change >2 and reads per million (RPM) >10. TargetScan and miRmap database were utilized to screen the targets of selected miRNAs. These miRNAs targets were further analyzed using IPA software (Ingenuity Systems, Redwood City, CA, USA) to understand the pathophysiological functions of miRNAs.

RNA extraction and RT-PCR

Extracellular vesicular RNAs of human and mouse urine (5 mL) were isolated using the Urine Exosome RNA Isolation Kit (47200, NORGEN, Canada), following the manufacturer's protocol. The cDNA was prepared by an oligo (dT) primer and RT (Takara, Shiga, Japan) after RNA extraction. miRNAs were reverse transcribed using the Mir-X miRNA First Strand Synthesis Kit (638313, Takara, Japan). Quantitative RNA and miRNA analysis was performed using SYBR Green on the StepOnePlus Real time PCR system (Applied Biosystems, Foster City, CA, USA). PCR reaction was carried out with the following temperature profile: 95°C for 10 min, followed by 40 cycles of 95°C for 15 s and 60°C for 1 min. Relative expression levels of the mRNA and miRNA in cells were normalized to GAPDH or U6, respectively. miRNAs in extracellular vesicles isolated from urine were normalized with cel-miR-39 (Exiqon, Vedbaek, Denmark) as a spike-in control and compared with a reference sample. The primers used are listed in Table S2. Relative expression was presented using the $2^{-\Delta\Delta Ct}$ method. cel-miR-39-3p was utilized as a candidate reference miRNA to normalize the data of qPCR and reduce non-biological variation in the data.[39]

Transient Transfection

SOCS5 siRNA (25 nM), siRNA-negative control (si-NC, 25 nM), miR-33-5p inhibitor (50 nM), miR-negative control of inhibitor (anti-miR-NC, 50 nM), miR-33-5p mimic (200 nM), and miR-negative control of mimic (miR-NC, 200 nM) (Dharmacon, USA) were transfected into cells by using Lipofectamine RNAiMAX Transfection Reagent (Invitrogen, USA), following the manufacturer's instructions.

Measurement of Cell Apoptosis by Flow Cytometry and Caspase-3 and -9 Activity

MMCs were cultured in NG and HG, with or without mouse recombinant Angpt2 protein (300 ng/mL), for 48 hr. To evaluate apoptosis, MMCs were double stained by using fluorescein isothiocyanate Annexin-V and propidium iodide (PI) assay kit (Cell Signaling Technology, USA), following the manufacturer's protocols. Samples were analyzed by flow cytometry (BD Accuri C6 Plus personal flow cytometer, Becton Dickinson, USA). Cell apoptosis was expressed as the percentage of cells with Annexin-V and PI double staining in total cell populations

Caspase-3 and -9 were detected by caspase-3 and -9 activity assay kit (BioVision Technologies, USA), following the manufacturer's instructions, and they were analyzed using a fluorescence plate reader, with excitation at 380 nm and emission at 420–460 nm.

Western Blot Analysis

MMCs were lysed in radioimmunoprecipitation assay (RIPA) lysis buffer (EMD Millipore, USA). Equal amounts of protein were subjected to 9%–11% SDS-PAGE for electrophoresis, followed by transfer onto an Immobilon-polyvinylidene fluoride (PVDF) membrane. Membranes were blocked with 5% blocking buffer and sequentially immunoblotted with each primary antibody overnight at 4°C. Membranes were washed with Tris-buffered saline (TBS) Tween-20, then incubated with an HRP-conjugated secondary antibody. Corresponding bands were detected using a chemiluminescence HRP substrate kit (Millipore, USA). The chemiluminescence signal was analyzed using Proteinsimple+Fluorchem Q system (Alpha Innotech, USA). The densitometry of the bands was analyzed using ImageJ software (USA).

Luciferase Reporter Assay

HEK293 cells (1×10^4/well) were seeded in 96-well plates and incubated for 24 hr before transfection. Cells were cotransfected with pGL3-SOCS5-3′ UTR luciferase plasmid/pRL-TK Renilla (1:8) or pGL3-SOCS5-3′ UTR MT luciferase plasmid/pRL-TK Renilla (1:8) with various miRNA mimics (control mimic or miR-33-5p mimic) by DharmaFECT Duo transfection regent (Promega, USA) after 48 hr. Both firefly and Renilla luciferase activities were quantified using the Dual-Glo Luciferase Assay System (Promega, USA), according to the manufacturer's instructions.

Immunohistochemistry Stain of Human and Mouse Kidneys

The kidney tissue sections were fixed in 4% paraformaldehyde for immunohistochemical staining. SOCS5 antibody (GTX104722) (GeneTex) and anti-alpha smooth muscle actin antibody (α-SMA; ab5694, Abcam) were co-stained.

Statistical Analysis

The continuous variables were expressed as mean ± SEM or median (25^{th} and 75^{th} percentiles), as appropriate. The categorical variables were expressed as percentages. Differences in the distribution of categorical variables were tested using the chi-square test. Skewed distribution continuous variables were log transformed to attain normal distribution. The association among continuous variables was examined by Spearman correlation. The significance of differences in continuous variables between groups was tested using Student's t test or one-way ANOVA, followed by the post hoc test adjusted with a Tukey correction, as appropriate.

SUPPLEMENTAL INFORMATION

Supplemental Information includes two tables and three figures and can be found with this article online at https://doi.org/10.1016/j.omtn.2018.10.003.

AUTHOR CONTRIBUTIONS

Conceptualization, Y.-C.T., M.-C.K., and Y.-L.H.; Methodology, Y.-L.H., P.-L.K., and M.-C.K.; Investigation, L.-Y.W.; Writing – Original Draft, Y.-C.T.; Writing – Review and Editing, M.-C.K. and Y.-L.H.; Funding Acquisition, Y.-C.T.; Resources, W.-W.H., P.-H.W., W.-A.C., M.-C.K., P.-L.K., and Y.-L.H.; Supervision, M.-C.K. and Y.-L.H.

CONFLICTS OF INTEREST

The authors have no conflicts of interest.

ACKNOWLEDGMENTS

The authors thank the Department of Pathology, Kaohsiung Municipal Ta-Tung Hospital and the Center for Research Resources and Development, Kaohsiung Medical University, Kaohsiung, Taiwan. This study was funded by grants from the Ministry of Science and Technology, Taiwan (MOST 107-2314-B-037-012, MOST 106-2314-B-037-055, MOST 105-2314-B-037-022 and MOST 104-2314-B-037-053-MY4), Kaohsiung Medical University, Kaohsiung, Taiwan (KMU-DK105007, KMU-DK106007, and KMU-DK108008), and Kaohsiung Medical University Hospital, Kaohsiung, Taiwan (KMUH105-5R22, KMUH106-6R26, KMUHS10701, and KMUHS10712).

REFERENCES

1. White, S.L., Cass, A., Atkins, R.C., and Chadban, S.J. (2005). Chronic kidney disease in the general population. Adv. Chronic Kidney Dis. *12*, 5–13.
2. Khera, T., Martin, J., Riley, S., Steadman, R., and Phillips, A.O. (2006). Glucose enhances mesangial cell apoptosis. Lab. Invest. *86*, 566–577.
3. Pesce, C., Menini, S., Pricci, F., Favre, A., Leto, G., DiMario, U., and Pugliese, G. (2002). Glomerular cell replication and cell loss through apoptosis in experimental diabetes mellitus. Nephron *90*, 484–488.
4. Mishra, R., Emancipator, S.N., Kern, T., and Simonson, M.S. (2005). High glucose evokes an intrinsic proapoptotic signaling pathway in mesangial cells. Kidney Int. *67*, 82–93.
5. Brindle, N.P., Saharinen, P., and Alitalo, K. (2006). Signaling and functions of angiopoietin-1 in vascular protection. Circ. Res. *98*, 1014–1023.
6. Hughes, D.P., Marron, M.B., and Brindle, N.P. (2003). The antiinflammatory endothelial tyrosine kinase Tie2 interacts with a novel nuclear factor-kappaB inhibitor ABIN-2. Circ. Res. *92*, 630–636.
7. Fiedler, U., and Augustin, H.G. (2006). Angiopoietins: a link between angiogenesis and inflammation. Trends Immunol. *27*, 552–558.
8. Fiedler, U., Scharpfenecker, M., Koidl, S., Hegen, A., Grunow, V., Schmidt, J.M., Kriz, W., Thurston, G., and Augustin, H.G. (2004). The Tie-2 ligand angiopoietin-2 is stored in and rapidly released upon stimulation from endothelial cell Weibel-Palade bodies. Blood *103*, 4150–4156.
9. Fiedler, U., Reiss, Y., Scharpfenecker, M., Grunow, V., Koidl, S., Thurston, G., Gale, N.W., Witzenrath, M., Rosseau, S., Suttorp, N., et al. (2006). Angiopoietin-2 sensitizes endothelial cells to TNF-alpha and has a crucial role in the induction of inflammation. Nat. Med. *12*, 235–239.
10. Oh, H., Takagi, H., Suzuma, K., Otani, A., Matsumura, M., and Honda, Y. (1999). Hypoxia and vascular endothelial growth factor selectively up-regulate angiopoietin-2 in bovine microvascular endothelial cells. J. Biol. Chem. *274*, 15732–15739.
11. van Meurs, M., Kümpers, P., Ligtenberg, J.J., Meertens, J.H., Molema, G., and Zijlstra, J.G. (2009). Bench-to-bedside review: Angiopoietin signalling in critical illness - a future target? Crit. Care *13*, 207.
12. Lim, H.S., Blann, A.D., Chong, A.Y., Freestone, B., and Lip, G.Y. (2004). Plasma vascular endothelial growth factor, angiopoietin-1, and angiopoietin-2 in diabetes: implications for cardiovascular risk and effects of multifactorial intervention. Diabetes Care *27*, 2918–2924.
13. Hammes, H.P., Lin, J., Wagner, P., Feng, Y., Vom Hagen, F., Krzizok, T., Renner, O., Breier, G., Brownlee, M., and Deutsch, U. (2004). Angiopoietin-2 causes pericyte dropout in the normal retina: evidence for involvement in diabetic retinopathy. Diabetes *53*, 1104–1110.
14. Tsai, Y.C., Lee, C.S., Chiu, Y.W., Lee, J.J., Lee, S.C., Hsu, Y.L., and Kuo, M.C. (2018). Angiopoietin-2, Renal Deterioration, Major Adverse Cardiovascular Events and All-Cause Mortality in Patients with Diabetic Nephropathy. Kidney Blood Press. Res. *43*, 545–554.
15. Chitwood, D.H., and Timmermans, M.C. (2007). Target mimics modulate miRNAs. Nat. Genet. *39*, 935–936.
16. Chen, Y.Q., Wang, X.X., Yao, X.M., Zhang, D.L., Yang, X.F., Tian, S.F., and Wang, N.S. (2012). Abated microRNA-195 expression protected mesangial cells from apoptosis in early diabetic renal injury in mice. J. Nephrol. *25*, 566–576.
17. Kato, M., Zhang, J., Wang, M., Lanting, L., Yuan, H., Rossi, J.J., and Natarajan, R. (2007). MicroRNA-192 in diabetic kidney glomeruli and its function in TGF-beta-induced collagen expression via inhibition of E-box repressors. Proc. Natl. Acad. Sci. USA *104*, 3432–3437.
18. Wang, Q., Wang, Y., Minto, A.W., Wang, J., Shi, Q., Li, X., and Quigg, R.J. (2008). MicroRNA-377 is up-regulated and can lead to increased fibronectin production in diabetic nephropathy. FASEB J. *22*, 4126–4135.
19. Kato, M., Arce, L., Wang, M., Putta, S., Lanting, L., and Natarajan, R. (2011). A microRNA circuit mediates transforming growth factor-β1 autoregulation in renal glomerular mesangial cells. Kidney Int. *80*, 358–368.
20. Park, J.T., Kato, M., Yuan, H., Castro, N., Lanting, L., Wang, M., and Natarajan, R. (2013). FOG2 protein down-regulation by transforming growth factor-β1-induced microRNA-200b/c leads to Akt kinase activation and glomerular mesangial hypertrophy related to diabetic nephropathy. J. Biol. Chem. *288*, 22469–22480.
21. Nassirpour, R., Mathur, S., Gosink, M.M., Li, Y., Shoieb, A.M., Wood, J., O'Neil, S.P., Homer, B.L., and Whiteley, L.O. (2014). Identification of tubular injury microRNA biomarkers in urine: comparison of next-generation sequencing and qPCR-based profiling platforms. BMC Genomics *15*, 485.
22. Kasinath, B.S., and Feliers, D. (2011). The complex world of kidney microRNAs. Kidney Int. *80*, 334–337.
23. O'Sullivan, L.A., Liongue, C., Lewis, R.S., Stephenson, S.E., and Ward, A.C. (2007). Cytokine receptor signaling through the Jak-Stat-Socs pathway in disease. Mol. Immunol. *44*, 2497–2506.
24. USRDS (2011). United States Renal Data System 2010 Annual Data Report: International Comparisons. Am. J. Kidney Dis. *57*, e383–e396.
25. Rizkalla, B., Forbes, J.M., Cao, Z., Boner, G., and Cooper, M.E. (2005). Temporal renal expression of angiogenic growth factors and their receptors in experimental diabetes: role of the renin-angiotensin system. J. Hypertens. *23*, 153–164.
26. Yamamoto, Y., Maeshima, Y., Kitayama, H., Kitamura, S., Takazawa, Y., Sugiyama, H., Yamasaki, Y., and Makino, H. (2004). Tumstatin peptide, an inhibitor of angiogenesis, prevents glomerular hypertrophy in the early stage of diabetic nephropathy. Diabetes *53*, 1831–1840.
27. Jenny Zhou, H., Qin, L., Zhang, H., Tang, W., Ji, W., He, Y., Liang, X., Wang, Z., Yuan, Q., Vortmeyer, A., et al. (2016). Endothelial exocytosis of angiopoietin-2 resulting from CCM3 deficiency contributes to cerebral cavernous malformation. Nat. Med. *22*, 1033–1042.
28. Davis, B., Dei Cas, A., Long, D.A., White, K.E., Hayward, A., Ku, C.H., Woolf, A.S., Bilous, R., Viberti, G., and Gnudi, L. (2007). Podocyte-specific expression of

angiopoietin-2 causes proteinuria and apoptosis of glomerular endothelia. J. Am. Soc. Nephrol. *18*, 2320–2329.

29. Fu, J., Lee, K., Chuang, P.Y., Liu, Z., and He, J.C. (2015). Glomerular endothelial cell injury and cross talk in diabetic kidney disease. Am. J. Physiol. Renal Physiol. *308*, F287–F297.

30. Huang, Y.Q., Li, J.J., Hu, L., Lee, M., and Karpatkin, S. (2002). Thrombin induces increased expression and secretion of angiopoietin-2 from human umbilical vein endothelial cells. Blood *99*, 1646–1650.

31. Hackett, S.F., Wiegand, S., Yancopoulos, G., and Campochiaro, P.A. (2002). Angiopoietin-2 plays an important role in retinal angiogenesis. J. Cell. Physiol. *192*, 182–187.

32. Schena, F.P., Serino, G., and Sallustio, F. (2014). MicroRNAs in kidney diseases: new promising biomarkers for diagnosis and monitoring. Nephrol. Dial. Transplant. *29*, 755–763.

33. Wu, H., Kong, L., Zhou, S., Cui, W., Xu, F., Luo, M., Li, X., Tan, Y., and Miao, L. (2014). The role of microRNAs in diabetic nephropathy. J. Diabetes Res. *2014*, 920134.

34. Yu, B., Li, W., Al, F., and Chen, Z. (2017). MicroRNA-33a deficiency inhibits proliferation and fibrosis through inactivation of TGF-β/Smad pathway in human cardiac fibroblasts. Pharmazie *72*, 456–460.

35. Lorenzen, J.M., and Thum, T. (2012). Circulating and urinary microRNAs in kidney disease. Clin. J. Am. Soc. Nephrol. *7*, 1528–1533.

36. Ortiz-Muñoz, G., Lopez-Parra, V., Lopez-Franco, O., Fernandez-Vizarra, P., Mallavia, B., Flores, C., Sanz, A., Blanco, J., Mezzano, S., Ortiz, A., et al. (2010). Suppressors of cytokine signaling abrogate diabetic nephropathy. J. Am. Soc. Nephrol. *21*, 763–772.

37. Chen, M., Wang, W., Ma, J., Ye, P., and Wang, K. (2016). High glucose induces mitochondrial dysfunction and apoptosis in human retinal pigment epithelium cells via promoting SOCS1 and Fas/FasL signaling. Cytokine *78*, 94–102.

38. Venieratos, P.D., Drossopoulou, G.I., Kapodistria, K.D., Tsilibary, E.C., and Kitsiou, P.V. (2010). High glucose induces suppression of insulin signalling and apoptosis via upregulation of endogenous IL-1beta and suppressor of cytokine signalling-1 in mouse pancreatic beta cells. Cell. Signal. *22*, 791–800.

39. Marabita, F., de Candia, P., Torri, A., Tegnér, J., Abrignani, S., and Rossi, R.L. (2016). Normalization of circulating microRNA expression data obtained by quantitative real-time RT-PCR. Brief. Bioinform. *17*, 204–212.